Available online at www.sciencedirect.com
SCIENCE DIRECT
Journal of Molecular Structure 702 (2004) 9–21
Journal of MOLECULAR STRUCTURE
www.elsevier.com/locate/molstruc

Simulation of IR and Raman spectra based on scaled DFT force fields: a case study of 2-(methylthio)benzonitrile, with emphasis on band assignment

V. Krishnakumar[a], Gábor Keresztury[b,*], Tom Sundius[c], R. Ramasamy[d]

[a]Department of Physics, Nehru Memorial College, Puthanampatti 621007, Tiruchirapalli, India
[b]Chemical Research Center, Hungarian Academy of Sciences, P.O. Box 17, H-1525 Budapest, Hungary
[c]Department of Physical Sciences, University of Helsinki, P.O. Box 64, FIN-00014 Helsinki, Finland
[d]Department of Physics, Shanmuga College of Engineering, SASTRA Deemed University, Thirumalaisamuthiram, Thanjavur 613402, India

Received 26 March 2004; revised 26 May 2004; accepted 1 June 2004

Abstract

The solid phase FT-IR and FT-Raman, solution phase linear dichroism IR (in nematic liquid crystal), and vapor phase GC/IR spectra of 2-(methylthio)benzonitrile have been recorded in the regions 4000–50, 3500–100, 4000–400, and 4000–650 cm^{-1}, respectively. The spectra were interpreted with the aid of normal coordinate analysis following full structure optimizations and force field calculations based on density functional theory (DFT) using standard B3LYP/6-31G* and B3LYP/6-311 + G** method and basis set combinations. Normal coordinate calculations were performed with the DFT force field corrected by a recommended set of scaling factors yielding fairly good agreement between observed and calculated frequencies. IR dichroism data revealed an error in band assignment associated with a νCS vibration, which could be eliminated only by introducing independent scaling factors for sulfur, whereas the overall frequency fit was further improved. Simulation of infrared and Raman spectra utilizing the results of these calculations led to excellent overall agreement with the observed spectral patterns, especially with the higher level basis set. The SQM approach applying selective scaling of the DFT force field was shown to be superior to the uniform scaling method in its ability to allow for making modifications in the band assignment, resulting in more accurate simulation of IR and Raman spectra including band polarizations and intensity patterns.

Keywords: Vibrational spectra; DFT calculations; SQM force field; IR and Raman intensities; IR linear dichroism; Vibrational assignment

1. Introduction

Vibrational spectroscopy is perhaps the most versatile and yet a relatively simple and cheap instrumental method of structural analysis that is applied in virtually all branches of chemistry. Thus, these days infrared spectra are routinely measured by organic chemists to check the formation of molecules with desired structures. However, as the structures of target molecules (and hence their spectra) become more and more complex, confirmation of the presence of specific structural moieties on the basis of empirical spectra–structure correlations alone [1] may become troublesome, even for an experienced spectroscopist. With the development of sophisticated but cost-effective computational methods of theoretical chemistry and the proliferation of ever more powerful personal computers, simulation of vibrational spectra based on quantum mechanical (QM) calculations can be of considerable help in structural identification. Since appropriate user-friendly software is increasingly available for such calculations, the use of these methods is becoming a realistic approach that can possibly be applied even by non-specialists. The results of such calculations, however, cannot always be taken as granted. With the present vibrational analysis of a relatively simple benzene derivative, 2-(methylthio)benzonitrile, we are going to show that mechanical application of QM methods without proper scaling of the computed force field may lead to

* Corresponding author. Fax: +36-1-3257554.
E-mail addresses: kergabor@chemres.hu (G. Keresztury), vkrishna_kumar@yahoo.com (V. Krishnakumar), tom.sundius@helsinki.fi (T. Sundius), ramasamy_ty@yahoo.co.in (R. Ramasamy).

0022-2860/$ - see front matter © 2004 Elsevier B.V. All rights reserved.
doi:10.1016/j.molstruc.2004.06.004

misassignment of some key spectral features, e.g. the C–S stretching band.

The philosophy of computational methods applied in vibrational spectroscopy changed significantly during the last two decades. The empirical simplified valence force fields used earlier for traditional normal coordinate analysis (NCA) [2] have been gradually replaced by full harmonic force fields obtained from ab initio quantum mechanical (QM) calculations [3–9]. With some QM program packages, vibrational frequencies and normal modes can be calculated as a matter of routine, and even the calculation of IR and Raman intensities has become feasible with the use of higher level methods taking into account electron correlations and large enough basis sets.

During the years sufficient experience has been accumulated with the application of various quantum mechanical methods and basis sets to vibrational studies [10,11]. There seems to be a general consensus that density functional theory (DFT), namely, the B3LYP method combining the 3-parameter exchange functional of Becke [12] with the Lee, Young, and Parr (LYP) correlation functional [13] yields sufficiently good and consistent results even with the standard 6-31G* basis set at moderate computational costs. Due to some systematic errors, however, some sort of empirical correction of the force field is required to obtain an acceptable agreement (in the order of 15–20 cm^{-1}) of observed and calculated frequencies. In simpler molecules *global scaling* (or uniform scaling) of the theoretical force field with one common scale factor may prove satisfactory [10]. It has been shown, however, that application of multiple scale factors, i.e. *selective scaling* of the ab initio calculated force field developed by Pulay et al. [14–16], leads to better results. In addition to correcting for overestimation of the force constants by the commonly used QM approaches, scaling of the force field can also absorb the effect of anharmonicity of normal vibrations. The different approaches of correcting the ab initio force fields have been reviewed and discussed recently by Panchenko [17,18]. One of the most successful selective scaling schemes, developed with a deep understanding of the nature of molecular vibrations, is the so-called SQM (scaled quantum mechanical) force field method [14–16]. It requires transformation of the QM force field to internal coordinates and applies a *limited number* of independent scaling factors that are common within groups of similar internal coordinates. Ideally, the number of scale factors applied is kept to a possible minimum to safeguard against arbitrariness in the effective force field produced. This sounds like justifying the use of global scaling which in practice means direct scaling of the calculated frequencies by a single factor, therefore appears to be much more attractive to those having little practice in normal coordinate calculations (since this way the tedious transformation to internal coordinates and the follow-up calculations can be skipped).

Uniform scaling (or frequency scaling) has been criticized by Pulay at al. [7] pointing out that no scaling and uniform scaling of the force field may often lead to misassignments in case of large molecules, since proper correction for systematic errors of theory is impossible by a single factor. To enhance the utility of the SQM force field method, a set of 11 transferable scaling factors have been proposed for use with the B3LYP/6-31G* density functional (DFT) force field that seem to be transferable within a wide range of organic molecules containing the atoms C, O, N, and H [15,16]. A significant advantage of the SQM force field method is that it does not require the analysis of isotopomer spectra to get an *approximately* correct assignment. However, depending on the level of QM calculation and the scale factors used, 'minor' mistakes such as exchanged assignment of close-lying bands cannot be excluded, especially in larger molecules containing various kinds of structural groups with overlapping regions of vibrational frequencies. The essence of vibrational analysis is to arrive at *correct and reliable* band assignments. To ensure this, they should be checked against IR and Raman selection rules and all available experimental data including relative intensities and, possibly, band polarizations as well. Successful spectral simulation cannot be expected, even at higher level of theory, without fine-tuning of band assignments by proper scaling of the force field, which may sometimes require introduction of additional scale factors for new kinds of internal coordinates like those containing heavier atoms.

From spectroscopists' point of view, 2-MTBN can be proposed as a suitable test molecule for SQM calculations: it is a relatively small molecule but contains carbon atoms of three different hybridization states and a sulfur atom which, as an element from the third row of the periodic table, may require individual scale factors, different from those of the second row elements [15,16]. Furthermore, in this molecule all basic types of internal coordinates can be found including a pair of linear bending coordinates that may present special interest.

The aim of this work is to check the performance of the B3LYP density functional force field for simulation of the IR and Raman spectra of 2-MTBN (that have not been subjected to vibrational analysis before) with the use of the standard 6-31G* and the large B3LYP/6-311 + G** basis sets, and comparing the effect of simpler and more elaborate versions of scaling, while paying attention to ensuring correct band assignments.

2. Experimental

The polycrystalline sample of 2-(methylthio)benzonitrile (2-MTBN) was kindly provided by Lancaster Synthesis (UK) and used as such for the spectral measurements. The room temperature Fourier transform infrared spectra of the title compound were measured in the 4000–50 cm^{-1} region

at a resolution of 1 cm^{-1} using a Bruker IFS 66V FTIR spectrometer equipped with dual detection: a cooled MCT detector for the mid-IR and a room temperature pyroelectric detector for the far IR range. The samples used in these measurements were KBr and polyethylene pellets, respectively. Boxcar apodization was used for the 250 averaged interferograms collected for both the sample and background.

The vapor phase IR spectrum was measured with a Nicolet Magna 750 FT-IR instrument connected to a Thermo Finnigan Trace™ gas chromatograph by means of a Thermo Nicolet GC-IR interface. The latter contained a 15-cm light pipe (flow-through capillary gas cell) and a high-sensitivity, narrow band MCT detector. The sample was injected into a Restek Rtx-5 type capillary column in the form of chloroform solution and eluted at 230 °C. The light pipe was held at 245 °C and the spectra were collected at 2 cm^{-1} resolution by accumulating 12 interferograms within the chromatographic peak of 2-MTBN. In addition to obtaining the vapor phase spectrum of the title compound, the GC-IR measurement was used to confirm the absence of any significant impurities.

The infrared linear dichroism (IR-LD) spectra of a nematic liquid crystalline solution of 2-MTBN (in ZLI-1695 supplied by Merck) were measured with the Nicolet Magna 750 FT-IR instrument in the 4000–400 cm^{-1} region at 2 cm^{-1} resolution by means of an Au/AgBr wire grid polarizer. Partial uniaxial orientation of the solute molecules in the LC solution was achieved at 6% (m/m) concentration in a specially prepared IR liquid cell of 0.25 mm path length [19]. The two polarized IR spectra obtained at 0 and 90 degree orientations of the electric vector with respect to the director of the nematic liquid crystal were analyzed by the stepwise reduction method [20,21] to distinguish between the bands of in-plane (A′) and out-of-plane (A″) modes.

The FT-Raman spectrum of the crystalline sample was recorded first with a Bruker IFS-66v model interferometer equipped with an FRA-106 FT-Raman accessory in the 3500–100 cm^{-1} Stokes region using the 1064 nm line of a Nd:YAG laser for excitation operating at 200 mW power. Further Raman measurements were done on a Nicolet Model 950 FT-Raman instrument under similar conditions after recrystallization of the sample from light petroleum. The latter spectrum had a flat background and showed much more spectral detail. For comparison with the simulated spectra, the observed spectrum was intensity corrected to eliminate distortions due to the frequency dependent instrument response. The reported wavenumbers are believed to be accurate within ± 1 cm^{-1}.

3. Computational details

Quantum chemical density functional calculations were carried out with the 1994 and 1998 versions of the GAUSSIAN suite of programs [22,23] using the B3LYP functionals [12,13] combined with the standard 6-31G* and 6-311 + G** basis sets (referred to as *small* and *large* basis sets, respectively). The Cartesian representation of the theoretical force constants has been computed at the optimized geometry by assuming C_s point group symmetry. Scaling of the force field was performed according to the SQM procedure [14,15] using selective (multiple) scaling in the natural internal coordinate representation [6,8]. Transformations of the force field and the subsequent normal coordinate analysis including the least-squares refinement of the scaling factors, calculation of total energy distribution (TED), and IR and Raman intensities were done on a PC with the MOLVIB program (version V7.0-G77) written by Sundius [24,25].

For the plots of simulated IR and Raman spectra, pure Lorentzian band shapes were used with a bandwidth (FWHH) of 7 cm^{-1}. During this process, the Raman activities (S_i) calculated with the GAUSSIAN-98 program and adjusted during the scaling procedure with MOLVIB were subsequently converted to relative Raman intensities (I_i) using the following relationship derived from the intensity theory of Raman scattering [26–28]:

$$I_i = \frac{f(\nu_0 - \nu_i)^4 S_i}{\nu_i\left[1 - \exp\left(-\frac{hc\nu_i}{kT}\right)\right]} \quad (1)$$

where ν_0 is the exciting frequency (in cm^{-1} units), ν_i is the vibrational wave number of the ith normal mode, h, c and k are fundamental constants, and f is a suitably chosen common normalization factor for all peak intensities.

4. Results and discussion

4.1. Molecular geometry

The two anticipated stable conformers of 2-(methylthio)-benzonitrile, both having C_s symmetry, are shown in Fig. 1. In accordance with our expectations, the DFT structure optimizations have shown that conformer **A** has a significantly lower energy than conformer **B**, the energy

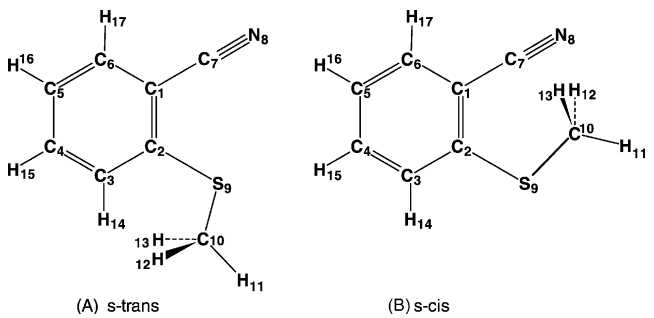

Fig. 1. The conformers considered and numbering of atoms of 2-MTBN; (A) stable s-*trans* conformation; (B) s-*cis* conformation corresponding to a saddle point.

Table 1
Optimized geometrical parameters of 2-(methylthio)benzonitrile obtained by B3LYP/6-31G* density functional calculations

Bond length	Value (Å)	Bond angle	Value (°)	Torsional angles	Value (°)
C1–C2	1.4181	C1–C2–C3	118.17	C2–S9–C10–H12	62.15
C2–C3	1.4009	C2–C3–C4	120.79	C2–S9–C10–H13	−62.15
C3–C4	1.3950	C3–C4–C5	120.87		
C4–C5	1.3956	C4–C5–C6	119.23		
C5–C6	1.3908	C2–C1–C7	120.68		
C1–C7	1.4337	C2–C1–N8	120.68		
C7–N8	2.5977	C3–C2–S9	124.13		
C2–S9	1.7775	C2–S9–C10	103.12		
S9–C10	1.8232	S9–C10–H11	105.13		
C10–H11	1.0928	S9–C10–H12	111.79		
C10–H12	1.0932	S9–C3–H13	111.79		
C10–H13	1.0932	C2–C3–H14	120.27		
C6–H14	1.0835	C3–C4–H15	119.14		
C6–H15	1.0866	C4–C5–H16	120.61		
C5–H16	1.0854				

difference being 2.68 kcal/mol. Subsequent force field and vibrational frequency calculations performed at the B3LYP/6-31G* level of theory for both optimized structures have revealed, however, that conformer **B** has a large imaginary frequency (57.3i cm^{-1}) corresponding to the internal rotation around the C_{ar}–S bond. This means that there is a single energy minimum along this torsional coordinate corresponding to conformer **A**, while conformer **B** is a first order saddle point on the potential energy surface.

The optimized geometrical parameters of the stable conformer **A** are presented in Table 1. The corresponding energy was calculated to be $E = -761.991045449$ Hartrees. In addition to assuming C_s symmetry, the only constraint applied during this structure optimization was to keep the C–C≡N bond angle linear.

4.2. Analysis of spectra and theoretical spectrum simulations

The title compound, 2-(methylthio)benzonitrile, has C_s symmetry and its 45 normal modes are distributed between the two symmetry species as

$$\Gamma_{\text{vib}} = 30\text{A}'[\text{IR}(x,y),\text{R}(p)] + 15\text{A}''[\text{IR}(z),\text{R}(dp)] \quad (2)$$

i.e. all the vibrations are active both in infrared absorption and Raman scattering. In the Raman spectrum the in-plane vibrations (A′) give rise to polarized bands while the out-of-plane ones (A″) give rise to depolarized bands (if measured in liquid or solution state).

The measured FT-IR and FT-Raman spectra of polycrystalline samples of 2-MTBN are presented in Fig. 2. The peak positions of observed IR and Raman bands are collected in Table 2 including the IR vapor phase data as well as those obtained from polarized IR measurements made in unisotropic liquid crystal solution. Our tentative band assignments based in part on known group frequency correlations [1,29,30] and supported by the normal mode calculations are also given in the last column. Considering the selection rules for an isolated molecule, the IR and Raman band positions should coincide. Data in Table 2 show that this is largely true for the majority of bands in solid phase as well; the deviations that may be due to crystal field effects do not exceed ± 2 cm^{-1}. The frequency values underlined in Table 2 are those chosen to represent the observed data in the least-squares refinement calculations. Although the use of vapor phase data is usually preferred for this purpose, the differences between the solid and vapor frequencies are not very significant for 2-MTBN (thanks to the absence of hydrogen bonding) and, unlike the vapor spectrum, the IR and Raman spectra of the solid supply a nearly full set of fundamental frequencies.

The assignment of observed bands is greatly facilitated by observation of the polarization behavior (linear dichroism) of IR absorption bands in the uniaxially oriented nematic liquid crystal solution. The most informative part of the reduced LD spectra is shown in Fig. 3: the bands pointing downwards in trace (b) undoubtedly belong to out-of-plane vibrations, while the weak features pointing upwards in trace (a) are all in-plane vibrations. Thus in the region of overlapping bands between 800 and 700 cm^{-1}, for instance, it is clear that the weak features at 722 and 779 cm^{-1} belong to in-plane modes, while the somewhat stronger 717 cm^{-1} band and the very strong absorption at 758 cm^{-1} belong to out-of-plane vibrations. Unfortunately, three of the four aromatic CH wagging bands could not be identified in the polarized spectra due to their extremely small intensity. We were also unable to identify experimentally the out-of-plane component of the methyl asymmetric bending vibration near 1450 cm^{-1} because of the interfering strong absorption of the LC solvent in this region.

Detailed description of vibrational modes can be given by means of normal coordinate analysis (NCA). For this purpose, the full set of 58 standard internal valence coordinates (containing 13 redundancies) were defined as given in Table 3. From these, a non-redundant set of local

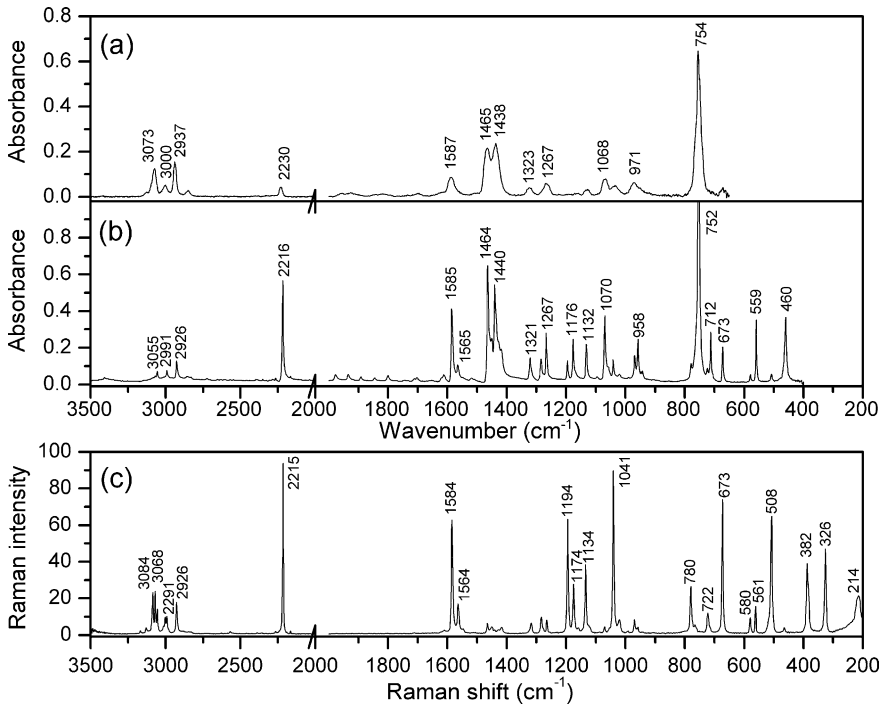

Fig. 2. Measured vibrational spectra of 2-MTBN: (a) vapor phase CG-IR spectrum; (b) FT-IR spectrum of a polycrystalline sample in KBr pellet; (c) near-IR excited FT-Raman spectrum of a pure polycrystalline sample.

internal coordinates were constructed (see Table 4) much like the 'natural internal coordinates' recommended by Fogarasi and Pulay [6,8]. The theoretically calculated DFT force fields were transformed to this latter set of vibrational coordinates and used in all subsequent calculations.

The effect of scaling was studied using the DFT force fields of the s-*trans* conformer of 2-MTBN. Several calculations were done with different kinds of scaling. The main differences between these calculations were as follows:

- Calculation *A* was done with the *unscaled* (raw) DFT force field transformed to natural internal coordinates;
- Calculation *B* was done after multiplying all elements of the above force field by a *single scale factor* of 0.919, a value obtained by a least-squares fit of 44 calculated frequencies of 2-MTBN to the observed ones. Note that this transformation is equivalent to uniform scaling of all calculated frequencies by 0.959;
- Calculation labeled C_0 was done with *selective scaling* according to the SQM scheme using 9 transferable scale factors from the recommended set [15] without refinement.
- In calculation C_{refined} the number of distinct scale factors was increased to 15 (as shown in the last columns of Table 4) and 14 of these were refined in a least-squares procedure to achieve a better frequency fit; for initial assignment of calculated frequencies to observed ones the increasing order obtained in calculation C_0 was used.
- Calculation D_{refined} consisted of a similar least-squares refinement of scale factors applied to the force field obtained with the large basis set (B3LYP/6-311 + G**).

The full results of these calculations are so voluminous that they cannot be presented here comprehensively. Instead, we have chosen to show some key aspects only, concentrating on the questions of frequency fit, differences in and correctness of band assignment, the quality of spectral simulations utilizing calculated IR and Raman intensities, and selected IR band polarizations.

The observed and calculated frequencies are compared for the above mentioned five calculations in Table 5, while the calculated IR and Raman intensities and normal mode descriptions (characterized by TED) are reported in Table 6 for the best approximations. For visual comparison, the observed and simulated FT-IR and FT-Raman spectra of 2-MTBN are presented in Figs. 4 and 5, respectively. The results of our analysis will be discussed in the next two subsections.

4.2.1. Effect of scaling on frequency fit and assignment

The vibrational frequencies calculated with the unscaled B3LYP/6-31G* force field (the 'raw' force field as obtained in the DFT calculation) are known to overestimate the experimental values by 2–5% on average. This is so in case of 2-MTBN as well, as reflected by calculation *A* in Table 5, with the RMS frequency error being 68.7 cm^{-1}. A tentative assignment is often made on the basis of unscaled computed frequencies by assigning the observed frequencies so that they are in the same (e.g. ascending) order as the calculated

Table 2
Frequencies (in cm^{-1}), relative intensities and polarizations of bands tentatively assigned to fundamental transitions in the observed vibrational spectra of 2-(methylthio)benzonitrile

No.	Infrared			Raman, solid[a]	Tentative assignments[b]
	Solid[a]	LC soln.[a,c]	Vapor[a]		
1	3091 vvw			*3091* sh, d	C–H stretching (20a)
2	3082 vvw			*3084* m	C–H stretching (2)
3	3069 vw		3073 m	*3068* m	C–H stretching (7b)
4	3055 w			*3055* m	C–H stretching (20b)
5	3002 sh		3000 w	*3001* m	CH_3 antisym. stretching
6	2991 w			*2991* m	CH_3 antisym. stretching
7	2926 w–m		2937 s	*2926* s	CH_3 sym. stretching
8	2216 s	2222 vs ‖	2230 w	*2215* vs	C≡N stretching
9	1585 s	1586 s ‖	1587 m	*1584* s	C–C stretching (8b)
10	1565 w	1564 w ‖		*1564* w	C–C stretching (8a)
11	*1464* s	1466 s ‖	1465 s	1465 w	C–H bending (19b)
12	*1450* sh	1447 s ‖		1450 w	CH_3 antisym. bending
13	*1440* s	1436 m (⊥)	1438 s	1440 sh	CH_3 antisym. bending
14	*1425* sh			1417 w	C–H bending (19a)
15	*1321* w–m	1322 w ‖	1323 w	1317 w	CH_3 sym. bending
16	*1284* w–m	1284 m ‖		1283 w	C–C stretching (14)
17	*1267* m	1265 m ‖	1267 m	1265 vw	C–H bending
18	1196 w–m	1196 w ‖		*1194* s	C–C stretching
19	*1176* m	1167 w ‖	1161 vw	1174 m	C–H bending (18a)
20	*1132* m	1130 m ‖	1128 w	1134 m	C–C stretching (13)
21	*1070* s	1072 m ‖	1068 m	1070 vw	Ring trigonal deformation (18b)
22	1041 w–m	1041 w ‖	1034 w	*1041* s	Ring breathing (1)
23	*989* vvw			991 vvw	C–H wagging (5)
24	*969* w–m	974 w–m ‖	971 w	969 w	(S)CH_3 rocking
25	*958* m	958 m (⊥)		958 vw	(S)CH_3 rocking
26	*942* sh		949 sh	941 vvw	C–H wagging (17b)
27	*853* vvw				C–H wagging (17a)
28	779 w	779 w ‖		*780* m	Ring deformation (12)
29	*752* vs	758 vs ⊥	754 vs		C–H wagging (11)
30	724 w	722 w ‖		*722* w	S–CH_3 stretching
31	*712* m	717 m ⊥	706 vvw	(712 sh)	Ring puckering (4)
32	673 m	673 m ‖	673 vw	*673* s	Ring deformation (6a)
33	579 w	576 w ‖	–	*580* w	C–C≡N bending
34	*559* s	559 m ⊥	–	561 w	Ring torsion (16a)
35	508 w		–	*508* s	Ring deformation (6b)
36	*460* s	466 m ⊥	–	464 vw	C_{ar}–S wagging (16b)
37			–	*387* m	Ring deformation (7a)
38	*382* w		–		Ring torsion (?)
39	326 w		–	*326* m	C–S–C bending
40			–	(230 sh,br)	Skeletal deformation (?)
41	*220* w		–	214 w,br	CH_3 torsion
42	*195* sh		–	(187 vw)	C–C(N) wagging (10a)
43	*146* m		–	148 m (?)	C–C≡N bending
44	*103* w		–	–	Ring torsion (10b)
45	?		–	–	C–S torsion

[a] Notation: vs, very strong; s, strong; m, medium; w, weak; vw, very weak; sh, shoulder; d, deconvolved component; wavenumbers in parentheses refer to uncertain values in case of very weak bands close to noise level; the underlined values were used as observed frequencies in scale factor refinements during the NCA calculations.

[b] The numbers in parentheses refer to the closest normal modes in benzene [29] numbered according to the Wilson-notation.

[c] IR linear dichroism measurements on oriented sample in nematic liquid crystal (LC) solution: ‖, in-plane polarization (A′); ⊥, out-of-plane polarization (A″).

ones. Then, for an easier comparison to the observed values, the calculated frequencies are multiplied by a common scale factor of less than 1, to decrease the overall deviation. In our case, the closest agreement with the application of a single scale factor can be achieved when the frequencies are multiplied by 0.959, which brings down the RMS error to 16.5 cm^{-1} (calculation *B*). This correction does not alter the order of calculated frequencies and leaves the calculated

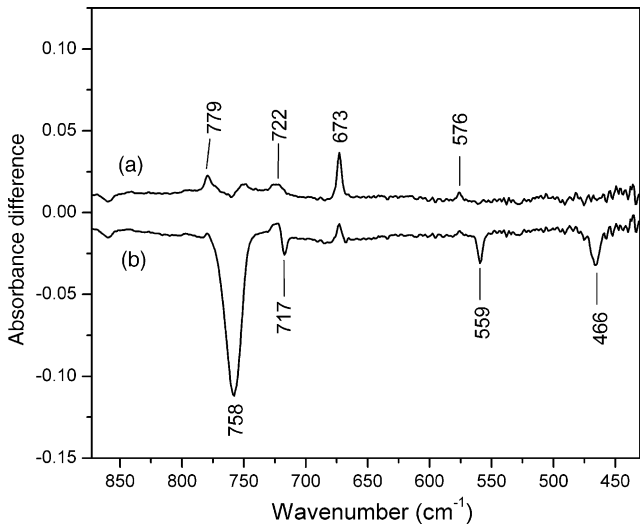

Fig. 3. Reduced IR-LD spectra of 2-MTBN observed in a nematic LC solution in the 850–450 cm^{-1} region: (a) reduced spectrum with the out-of-plane bands eliminated and the in-plane bands pointing upwards; (b) reduced spectrum with the out-of-plane bands pointing downwards.

normal modes unchanged; however, the assignments of some close-lying bands may not be correct (they may be interchanged) and the associated normal modes may differ from the true ones.

Using the set of transferable scale factors recommended by Rauhut and Pulay [15] (for the actual values see the column headed C_0 in Table 4), the RMS error in frequencies became 12.2 cm^{-1}, which permitted an easy assignment of most of the normal modes. Then, since the molecule under study contained a methyl group attached to sulfur and a nitrile group with linear bending vibrations (functional groups possibly underrepresented in the pool of data used in Ref. [6]), an attempt was made to refine the scale factors. A least-squares refinement of 14 of the 15 scale factors resulted in a mean deviation of 6.3 cm^{-1} between the experimental and calculated frequencies (calculation $C_{refined}$). The corresponding set of refined scale factors are given in the last column of Table 4.

It should be mentioned here that the results of least-squares refinement calculations depend on the observed frequencies (assigned as fundamentals) and on the starting values of the scale factors determining the zero-order calculated frequencies, i.e. on the initial band assignments. Initially there were uncertainties in the choice of observed frequencies due to appearance of some overtones and combination bands that could be mistaken for fundamental transitions in the following regions:

(a) A weak band observed at 3128 cm^{-1} in the Raman and vapor IR spectra was first assigned to ν_1, in spite of the fact that it seemed a little high for an aromatic CH stretch;
(b) The initial SQM calculations predicted *four* bands in the 1470–1400 cm^{-1} region ($\nu_{11}-\nu_{14}$), while in the IR crystal spectrum two strong bands and further five weak components were revealed by Fourier self-deconvolution, making the choice ambiguous;
(c) Three aromatic CH wagging modes could hardly be identified in the 1000–800 cm^{-1} region where a prominent, well resolved doublet was assigned to the split CH_3 wagging vibrations; ν_{23} (an aromatic CH wagging mode) was predicted at 985 cm^{-1} with nearly zero intensity in both IR and Raman spectra. Although an extremely weak feature was found near there in both observed spectra, accepting it for ν_{23} left a more prominent weak band at 1020 cm^{-1} unassigned;
(d) There was an uncertainty in assignment of the S–C(methyl) stretching vibration which was expected to give rise to a strong Raman band around 700 cm^{-1} [30];

Table 3
Definition of internal valence coordinates of 2-(methylthio)benzonitrile

No. (i)	Symbol	Type	Definition
Stretching			
1–4	r_i	C–H (aromatic)	C3–H14, C4–H15, C5–H16, C6–H17
5–7	r_i	C–H (methyl)	C10–H11, C10–H12, C10–H13
8–9	Q_i	C–S, S–C (methyl)	C2–S9, C10–S9
10–15	R_i	C–C (aromatic)	C1–C2, C2–C3, C3–C4, C4–C5, C5–C6
16	P_i	C–C (substitution)	C1–C7
17	T_i	C≡N	C7–N8
Bending			
18–25	β_i	C–C–H	C4–C3–H14, C2–C3–H14, C5–C4–H15, C3–C4–H15, C6–C5–H16, C4–C5–H16, C1–C6–H17, C5–C6–H17
26–28	β_i	S–C–H	S9–C10–H11, S9–C10–H12, S9–C10–H13
29–31	α_i	H–C–H	H11–C10–H12, H11–C10–H13, H12–C10–H13
32–33	γ_i	C–C–C	C2–C1–C7, C6–C1–C7
34–35	δ_i	C–C–S	C3–C2–S9, C1–C2–S9
36	σ_i	C–S–C	C2–S9–C10
37–42	γ_i	C–C–C	C6–C1–C2, C1–C2–C3, C2–C3–C4, C3–C4–C5, C4–C5–C6, C5–C6–C1
Linear bending			
43–44	π_i	C–C≡N	C1–C7–N8 (in–plane), C1–C7–N8 (out–of–plane)
Out-of-plane bending (wagging)			
45–48	ω_i	C_{ar}–H	H14–C3–C4–C2, H15–C4–C5–C3, H16–C5–C6–C4, H17–C6–C1–C5
49	ω_i	C_{ar}–S	S9–C2–C3–C1
50	ω_i	C_{ar}–C	C7–C1–C2–C6
Torsion			
51	τ_i	τ C_{ar}–S	(C1, C3)–C2–S9–C10
52	τ_i	τ S–CH_3	C2–S9–C10–(H11, H12, H13)
53–58	τ_i	τ C–C (ring)	C5–C6–C1–C2, C6–C1–C2–C3, C1–C2–C3–C4, C2–C3–C4–C5, C3–C4–C5–C6, C4–C5–C6–C1

Table 4
Definition of local symmetry coordinates and the values of corresponding scale factors (s_i) used to correct the B3LYP/6-31G* (C_0, $C_{refined}$) and B3LYP/6-311 + G** ($D_{refined}$) force fields

No. (i)	Symbol[a]	Definition[b]	Scale factors used in calculations			
			Notation	C_0	$C_{refined}$	$D_{refined}$
1–4	CH_{ar}	r_1, r_2, r_3, r_4	s_1	0.920	0.914	0.9265
5	CH_3ss	$(r_5 + r_6 + r_7)/\sqrt{3}$	$s_1 \rightarrow s_{10}$	0.920	0.904	0.919
6	CH_3ips	$(2r_5 - r_6 - r_7)/\sqrt{6}$	$s_1 \rightarrow s_{10}$	0.920	0.904	0.919
7	CH_3ops	$(r_6 - r_0)/\sqrt{2}$	$s_1 \rightarrow s_{10}$	0.920	0.904	0.919
8–9	$C_{ar}S$, SC	Q_8, Q_9	$s_2 \rightarrow s_{11}$	0.922	1.003	1.024
10–15	CC_{ar}	R_{10}, R_{11}, R_{12}, R_{13}, R_{14}, R_{15}	s_2	0.922	0.929	0.954
16	CC	P_{16}	s_2	0.922	0.929	0.954
17	C ≡ N	T_{17}	$s_2 \rightarrow s_{12}$	0.922	0.892	0.901
18–21	bCH	$(\beta_{18} - \beta_{19})/\sqrt{2}, (\beta_{20} - \beta_{21})/\sqrt{2}, (\beta_{22} - \beta_{23})/\sqrt{2}, (\beta_{24} - \beta_{25})/\sqrt{2}$	s_3	0.950	0.943	0.977
22	CH_3sb	$(-\beta_{26} - \beta_{27} - \beta_{28} + \alpha_{29} + \alpha_{30} + \alpha_{31})/\sqrt{6}$	s_4	0.915	0.917	0.9405
23	CH_3ipb	$(-\alpha_{29} - \alpha_{30} + 2\alpha_{31})/\sqrt{6}$	s_4	0.915	0.917	0.9405
24	CH_3opb	$(\alpha_{29} - \alpha_{30})/\sqrt{2}$	s_4	0.915	0.917	0.9405
25	SCH_3ipr	$(2\beta_{26} - \beta_{27} - \beta_{28})/\sqrt{6}$	$s_3 \rightarrow s_{13}$	0.950	0.918	0.938
26	SCH_3opr	$(\beta_{27} - \beta_{28})/\sqrt{2}$	$s_3 \rightarrow s_{13}$	0.950	0.918	0.938
27	bCC	$(\gamma_{32} - \gamma_{33})/\sqrt{2}$	s_5	0.990	0.986	0.966
28	bCS	$(\delta_{34} - \delta_{35})/\sqrt{2}$	$s_5 \rightarrow s_{14}$	0.990	1.024	1.009
29	bCSC	σ_{36}	$s_5 \rightarrow s_{14}$	0.990	1.024	1.009
30	Rtrigd	$(\gamma_{37} - \gamma_{38} + \gamma_{39} - \gamma_{40} + \gamma_{41} - \gamma_{42})/\sqrt{6}$	s_5	0.990	0.986	0.966
31	Rsymd	$(-\gamma_{37} - \gamma_{36} + 2\gamma_{39} - \gamma_{40} - \gamma_{41} + 2\gamma_{42})/\sqrt{12}$	s_5	0.990	0.986	0.966
32	Rasyd	$(\gamma_{37} - \gamma_{38} + \gamma_{40} - \gamma_{41})/2$	s_5	0.990	0.986	0.966
33	bCCNip	π_{43}	s_6	0.913	0.958	0.961
34	bCCNop	π_{44}	s_6	0.913	0.958	0.961
35–38	gCH	ω_{45}, ω_{46}, ω_{47}, ω_{48}	s_7	0.976	0.967	0.962
39	gCC	ω_{50}	s_7	0.976	0.967	0.962
40	gCS	ω_{49}	$s_7 \rightarrow s_{15}$	0.976	0.934	1.007
41	tCS	τ_{51}	s_8 (fixed)	0.831	(0.831)	(0.831)
42	tCH_3	τ_{52}	s_8 (fixed)	0.831	(0.831)	(0.831)
43	tRtrig	$(\tau_{53} - \tau_{54} + \tau_{55} - \tau_{56} + \tau_{57} - \tau_{58})/\sqrt{6}$	s_9	0.935	0.936	0.896
44	tRsym	$(\tau_{53} - \tau_{55} + \tau_{56} - \tau_{58})/2$	s_9	0.935	0.936	0.896
45	tRasy	$(-\tau_{53} + 2\tau_{54} - \tau_{55} - \tau_{56} + 2\tau_{57} - \tau_{58})/\sqrt{12}$	s_9	0.935	0.936	0.896

[a] These symbols are used for description of the normal modes by TED in Table 6.
[b] The internal coordinates used here are defined in Table 3.

(e) The lowest frequency normal mode, the torsion around the C_{ar}–S bond (ν_{45}) was expected to be below 100 cm^{-1}, outside the spectral region covered by our instruments.

The results of both least-squares refinements *C* and *D* depended on the choice of observed frequencies in the above mentioned regions of uncertainty, thus several versions of assignment were tested until the best fit with reasonable scaling was found. The force fields corresponding to both basis sets gave an excellent frequency fit after refinement of the scale factors (see Table 5), with the large basis set performing only slightly better than the small one (the RMS frequency errors being 6.3 and 5.5 cm^{-1}, respectively), with almost exactly the same assignments. Thus, calculation $C_{refined}$ performed at B3LYP/6-31G* level can be regarded the method of choice for most practical applications. Because of this, a few key points of the band assignment and comparison with the uniform scaling calculation C_0 deserve further discussion.

The refinement produced slightly different scale factors for the aromatic and S-methyl CH stretches. The frequency fit of the three well defined aromatic CH stretching bands observed in Raman scattering (at 3055, 3069, and 3084 cm^{-1}) was almost perfect and the fourth such band was calculated at 3094 cm^{-1}. A new look at the Raman spectrum using Fourier self-deconvolution revealed a hidden band component at 3091 cm^{-1} which was then accepted for ν_1; confirmation came from IR in the form of a very-very weak feature at exactly the same frequency. (The weak Raman band observed at 3128 cm^{-1} was then reassigned as an overtone of ν_{10} (2×1564), and another one at 3167 was assigned to $2\nu_9$ (2×1584).)

The antisymmetric stretching vibrations of the S-methyl group that would be degenerate under C_{3v} local symmetry are split at a C_s site into two components observed at 3001 and 2991 cm^{-1} in the solid phase Raman spectrum. The SQM calculation reproduces both the frequencies and their splitting very well, attesting also that the higher frequency component belongs to the in-plane while the lower frequency to the out-of-plane $\nu_{as}CH_3$ mode. The splitting is equally well

Table 5
Comparison of observed and calculated frequencies (in cm^{-1}) of fundamental vibrations of 2-(methylthio)benzonitrile obtained by various types of scaling of DFT force fields B3LYP/6-31G* and B3LYP/6-311 + G**

i	Symm. species, C_s	Obsd. freqs.[a] ν_i^{obs}	Calculated frequencies and their deviations from observed data[b]									
			A, B3LYP/6-31G* (no scaling), $s_0 = 1.000$		*B*, B3LYP/6-31G*, uniform scaling[c], $s_0 = 0.919$		C_0, B3LYP/6-31G*, 9 scale factors fixed (from Ref. [16])[d]		$C_{refined}$, B3LYP/6-31G*, 14 scale factors refined[d]		$D_{refined}$, B3LYP/6-311 + G**, 14 scale factors refined[e]	
			ν_i^{calc}	$\Delta\nu_i$	ν_i^{calc}	$\Delta\nu_i$	ν_i^{calc}	$\Delta\nu_i$	ν_i^{calc}	$\Delta\nu_i$	ν_i^{calc}	$\Delta\nu_i$
1	A′	**3091**	3235	144	3102	11	3103	12	3093	2	3093	2
2	A′	**3084**	3224	140	3090	6	3092	8	3082	−2	3082	−2
3	A′	**3069**	3210	141	3077	8	3079	10	3069	0	3069	0
4	A′	**3055**	3195	140	3063	8	3065	10	3055	0	3055	0
5	A′	**3001**	3162	161	3031	30	3033	32	3006	5	3004	3
6	A″	**2991**	3153	162	3022	31	3024	33	2997	6	2997	6
7	A′	**2926**	3067	141	2940	14	2942	16	2915	−11	2916	−10
8	A′	**2215**	2341	126	2244	29	2247	32	2215	0	2215	0
9	A′	**1584**	1644	60	1576	−8	1589	5	1592	8	1592	8
10	A′	**1564**	1616	52	1550	−14	1563	−1	1566	2	1564	0
11	A′	**1464**	*1504* ↓	40	*1442* ↓	−22	1464	0	1464	0	1467	3
12	A′	**1450**	*1518* ↑	68	*1455* ↑	5	1448	−2	1448	−2	1443	−7
13	A″	**1440**	1502	62	1439	−1	1438	−2	1438	−2	1439	−1
14	A′	**1425**	1481	56	1420	−5	1437	12	1436	11	1425	0
15	A′	**1321**	1392	71	1335	14	1345	24	1333	12	1324	3
16	A′	**1284**	1335	51	1280	−4	1284	0	1288	4	1285	1
17	A′	**1267**	1303	36	1249	−18	1265	−2	1265	−2	1272	5
18	A′	**1195**	1222	27	1172	−23	1183	−12	1183	−12	1188	−7
19	A′	**1175**	1204	29	1154	−21	1170	−5	1168	−7	1176	1
20	A′	**1133**	1158	25	1111	−22	1120	−13	1125	−8	1130	−3
21	A′	**1070**	1091	21	1046	−24	1069	−1	1072	2	1070	0
22	A′	**1041**	1067	26	1023	−18	1031	−10	1035	−6	1039	−2
23	A″	**989**	*992* ↓	3	*951* ↓	−38	985	−4	979	−10	989	0
24	A′	**969**	*1005* ↑	36	*964* ↑	−5	979	10	966	−3	964	−5
25	A″	**958**	990	32	949	−9	964	6	949	−9	952	−6
26	A″	**942**	955	13	915	−27	946	4	941	−1	944	2
27	A″	**853**	875	22	838	−15	865	12	861	8	859	6
28	A′	**780**	791	11	759	−21	774	−6	778	−2	777	−3
29	A″	**753**	770	17	739	−14	760	7	757	4	753	0
30	A′	**723**	*725* ↓	2	*695* ↓	−28	*698* ↓	−25	725	2	724	1
31	A″	**712**	*733* ↑	21	*703* ↑	−9	*713* ↑	1	711	−1	717	5
32	A′	**673**	684	11	655	−18	670	−3	676	3	674	1
33	A′	**580**	587	7	563	−17	573	−7	579	−1	587	7
34	A″	**559**	581	22	557	−2	562	3	565	6	561	2
35	A′	**508**	516	8	495	−13	504	−4	508	0	508	0
36	A″	**460**	476	16	456	−4	464	4	461	1	460	0
37	A″	**387**	396	9	379	−8	381	−6	383	−4	383	−4
38	A′	**382**	386	4	370	−12	378	−4	383	1	375	−7
39	A′	**326**	328	2	314	−12	322	−4	328	2	328	2
40	A″	**230**	249	19	239	9	230	0	229	−1	223	−7
41	A′	**220**	217	−3	208	−12	215	−5	219	−1	215	−5
42	A″	**195**	195	0	187	−8	189	−6	188	−7	185	−10
43	A′	**146**	127	−19	122	−24	124	−22	126	−20	127	−19
44	A″	**103**	119	16	114	11	116	13	116	13	112	9
45	A″	?	52	–	50	–	47	–	47	–	49	–
RMS frequency error:				68.7		16.5		12.2		6.3		5.5

The observed frequencies are arranged in strictly decreasing order, while the calculated ones by unchanged assignment within each row. Arrows (↑ and ↓) next to some calculated values indicate interchanged order of calculated frequencies, i.e. interchanged assignments.

[a] Values taken from solid phase IR and Raman spectra.

[b] For band assignments by TED see Table 6.

[c] The optimized value of the single scale factor $s_0 = 0.919$ was obtained by least-squares refinement.

[d] For initial (fixed) and final (refined) values of scale factors see the columns headed C_0 and $C_{refined}$ in Table 4.

[e] For optimized values of the scale factors applied see the column headed $D_{refined}$ in Table 4.

Table 6
Assignment of fundamental vibrations of 2-(methylthio)benzonitrile by normal mode analysis based on SQM force field calculations using selectively scaled B3LYP/6-311 + G** force field

No. i	Sym. C_s	Observed fundamentals		Calculation D_{refined} (scaled B3LYP/6-311 + G** force field)			
		IR	Raman	ν_i	A_i, IR[a]	I_i, Raman[b]	TED (%) among types of internal coordinates[c]
1	A′	3091 vvw	3091 sh	3093	0.089	8.96	CH_{ar} (99)
2	A′	3082 vvw	3084 m	3082	0.128	13.90	CH_{ar} (99)
3	A′	3069 vw	3068 m	3069	0.077	7.34	CH_{ar} (99)
4	A′	3055 w	3055 m	3055	0.051	5.72	CH_{ar} (99)
5	A′	3002 sh	3001 m	3004	0.051	8.18	CH_3ips (98)
6	A″	2991 w	2991 m	2997	0.129	4.99	CH_3ops (100)
7	A′	2926 w–m	2926 s	2916	0.363	15.89	CH_3ss (98)
8	A′	2216 s	2215 vs	2215	0.609	70.80	CN (87), CC (12)
9	A′	1585 s	1584 s	1592	0.527	30.86	CC_{ar} (64), bCH (23), Rasyd (10)
10	A′	1565 m	1564 w	1564	0.128	6.66	CC_{ar} (67), bCH (21)
11	A′	1464 s	1465 w	1467	0.444	3.65	bCH (50), CC_{ar} (36)
12	A′	1450 sh	1450 w	1443	0.359	0.58	bCH (63), CC_{ar} (30)
13	A″	1440 s	1440 sh	1439	0.746	2.33	CH_3ipb (86)
14	A′	1425 sh	1417 w	1425	0.199	5.58	CH_3opb (96)
15	A′	1321 w–m	1317 w	1324	0.014	1.25	CH_3sb (93)
16	A′	1284 w–m	1283 w	1285	0.184	7.88	CC_{ar} (86)
17	A′	1267 m	1265 vw	1272	0.130	2.33	bCH (54), CC_{ar} (25)
18	A′	1196 w–m	1194 s	1188	0.061	24.05	CC (30), CC_{ar} (30), bCH (23), Rtrigd (11)
19	A′	1176 m	1174 w	1176	0.028	6.41	bCH (76), CC_{ar} (23)
20	A′	1132 m	1134 m	1130	0.162	17.40	CC_{ar} (45), bCH (33), C_{ar}S (12)
21	A′	1070 s	1070 vw	1070	0.346	0.35	Rtrigd (52), CC_{ar} (19), C_{ar}S (13)
22	A′	1041 w–m	1041 s	1039	0.263	41.91	CC_{ar} (71), bCH (12)
23	A″	989 vvw	991 vvw	989	0.000	0.07	gCH (86), tRtrig (12)
24	A′	969 w–m	969 w	964	0.091	3.37	CH_3ipr (86)
25	A″	958 m	958 vw	952	0.037	0.05	gCH (89)
26	A″	942 sh	941 vvw	944	0.046	1.60	CH_3opr (92)
27	A″	853 vvw		859	0.004	1.19	gCH (83)
28	A′	779 w	780 m	777	0.099	10.74	Rasyd (34), Rtrigd (19), CC (16), C_{ar}S (10)
29	A″	752 vs		753	1.000	1.68	gCH (80)
30	A′	724 w	722 w	724	0.006	5.54	SC (86)
31	A″	712 m	(712 sh)	717	0.184	2.25	tRtrig (51), gCS (16), gCC (16), gCH (12)
32	A′	673 m	673 s	674	0.122	18.15	Rsymd (48), C_{ar}S (16), CC_{ar} (14)
33	A′	579 w	580 w	587	0.015	4.69	bCC (41), bCCNip (38), CC_{ar} (11)
34	A″	559 s	561 w	561	0.056	1.63	tRtrig (36), bCCNop (19), tRasy (16), gCH (15), gCC (12)
35	A′	508 w	508 s	508	0.026	21.33	Rsymd (32), CC (16), CC_{ar} (14), C_{ar}S (13)
36	A″	460 s	464 vw	460	0.148	2.16	gCS (35), tRasy (23), tRsym (21)
37	A″		387 m	383	0.026	7.10	Rasyd (41), C_{ar}S (25), bCSC (14)
38	A′	382 w		375	0.007	4.80	tRsym (56), bCCNop (13), tRasy (12), gCH (11)
39	A′	326 w	326 m	328	0.025	25.26	bCSC (34), bCS (31), bCCNip (14)
40	A″		(230 sh,br)	223	0.001	0.48	tCH_3 (71)
41	A′	220 w	214 w,br	215	0.036	15.43	bCSC (45), bCS (31), bCCNip (11)
42	A″	195 sh	(187 vw)	185	0.004	4.24	gCC (25), tRsym (20), gCS (18), tCH_3 (13), bCCNop (11)
43	A′	146 m	148 m (?)	127	0.076	100.00	bCC (45), bCCNip (38), bCS (13)
44	A″	103 w	–	112	0.021	26.78	tRasy (55), bCCNop (13), tRtrig (10)
45	A″	?	–	49	0.023	12.80	tCS (73), tCH_3 (21)

[a] Relative absorption intensities normalized with the highest peak absorbance equal to 1.0.
[b] Relative Raman intensities calculated by Eq. (1) and normalized to 100.
[c] For the notation used see Table 4. Abbreviations used: R, ring; ss, symmetric stretching; ip, in-plane; op, out-of-plane; ips, in-plane stretching; ops, out-of-plane stretching; b, bending; sb, symmetric bending; ipb, in-plane bending; opb, out-of-plane bending; d, deformation; ipr, in-plane rocking; opr, out-of-plane rocking; asy, asymmetric, sym-symmetric; g, wagging; t, torsion; trig, trigonal.

reproduced when using uniform scaling (calculation *B*), but the frequencies are put well above 3000 cm^{-1}, into the region of aromatic CH stretching vibrations.

The assignment of the highly characteristic nitrile stretching mode (νC≡N) to the band at 2215 cm^{-1} is quite obvious in all calculations. The degenerate pair of linear bending vibrations of the C–C≡N moiety are split into in-plane and out-of-plane components, both strongly mixed with several other in-plane and out-of-plane vibrations, respectively, and contribute to several normal modes in the 600–100 cm^{-1} range (see Table 6). In the final force field, the in-plane linear bend has a smaller force

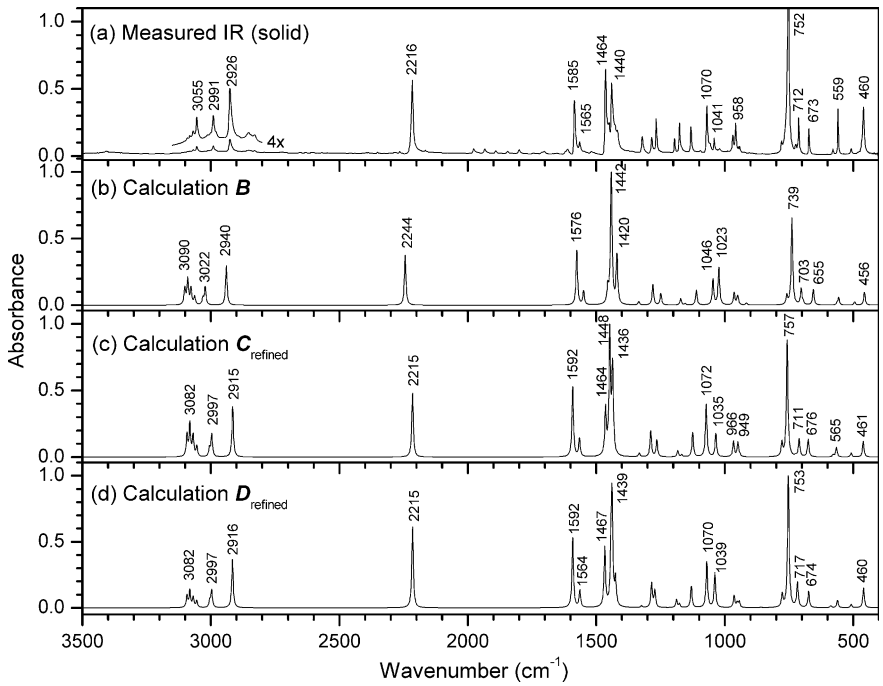

Fig. 4. Comparison of observed and calculated infrared spectra of 2-MTBN: (a) observed in solid state; (b) calculated using uniform scaling (calculation *B*); (c) calculated with B3LYP/6-31G* force field using selective scaling (calculation C_{refined}); (d) calculated with B3LYP/6-311 + G** force field using selective scaling (calculation D_{refined}).

constant (0.30 N/cm) than the out-of-plane counterpart (0.37 N/cm), which may be due to stronger interaction of the latter with the π-electrons of the aromatic ring.

The (S)CH_3 bending modes appear to be fairly pure group vibrations in both the uniform and selective scaling calculations. There is no question about the assignment of the CH_3 symmetric bending at 1325 cm^{-1}, but the split pair of asymmetric bending vibrations overlap in frequency with two aromatic CH bending vibrations. In this region, selective scaling *interchanges* the two highest frequency

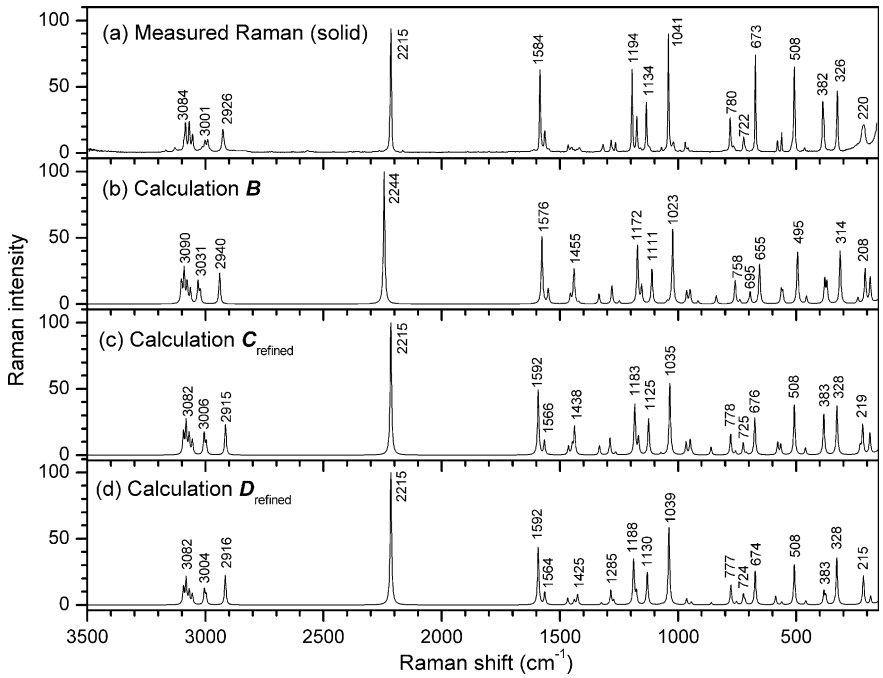

Fig. 5. Comparison of observed and calculated *Raman* spectra of 2-MTBN: (a) observed in solid state; (b) calculated using uniform scaling (calculation *B*); (c) calculated with B3LYP/6-31G* force field using selective scaling (calculation C_{refined}); (d) calculated with B3LYP/6-311 + G** force field using selective scaling (calculation D_{refined}).

modes: ν_{41}, a mainly aromatic CH bending mode, and ν_{40}, the in-plane component of the methyl asymmetric bending mode (CH_3ipb). The latter is shown to be a fairly pure group vibration by the SQM method, while it has stronger coupling with aromatic ring vibrations according to the uniform scaling calculation.

There are similar changes in the region of the (S)CH_3 rocking modes, between 1000 and 950 cm^{-1}. All frequency calculations show that the two rocking modes split under C_s symmetry by 15–18 cm^{-1} and that there are two aromatic CH out-of-plane bending (or CH wagging, ωCH) modes in the same region. Comparing the results of calculations *B* and C_0, the original order of the highest frequency CH wagging mode and the in-plane (S)CH_3 rocking vibration get interchanged in C_0 when the recommended selective scaling [15] is applied.

The interchanged assignment of a third pair of bands, the S–C(methyl) stretching mode and the ring puckering (trigonal torsion) of the aromatic ring in the vicinity of 700 cm^{-1}, can be eliminated only by introduction of new scale factor (e.g. s_{11}, see Table 4) and correction of the initial assignments in view of the observed IR band polarization properties.

4.2.2. *Effect of scaling on prediction of IR and Raman intensities*

With uniform scaling of the force field, the calculated intensity patterns of simulated spectra do not change, since uniform scaling does not change the vibrational modes, only decreases the frequencies in a proportional manner. Selective scaling, on the contrary, changes not only the frequencies but the normal modes of vibrations (the vibrational eigenvectors) and the corresponding total energy distributions (TED), too, which can give rise to changes in relative band intensities as well. This is exactly what can be seen in the above-mentioned regions of 2-MTBN spectra in Figs. 4 and 5, comparing panes (b) and (c). Careful comparison of the simulated IR spectra in Fig. 4 to the measured spectrum in Fig. 4(a), especially in the region below 1100 cm^{-1}, leads to the conclusion that the spectrum obtained by multiple scaling reproduces the measured intensity patterns noticeably better than the uniform scaling calculation. This, in turn, verifies the correctness of the assignment based on multiple scaling of the force field.

More solid evidence came from IR polarization data confirming the assignment of the out-of-plane bands. There was no doubt that the strong band at 752 cm^{-1} belonged to an out-of-plane mode, the in-phase wagging vibration of the four adjacent hydrogen atoms on the aromatic ring. But it could be established only by the measured band polarizations (see Fig. 3) that the very weak IR band at 722 cm^{-1} belonged to an in-plane mode (S–C stretch), while the stronger band at 712 cm^{-1} to an out-of-plane vibration (ring puckering). Since the assignments based on calculations *B* and C_0 gave a reverse assignment (see Table 5), the scale factors of the $S-C_{methyl}$ and $C_{ar}-S$ stretching force constants were allowed to change independently from those of other skeletal bonds and the starting assignment (pairing of observed and zero order calculated frequencies) was interchanged as well. As a result, calculation $C_{refined}$ supplied a new scale factor for the C–S bond stretches and led to correct assignment for the two bands in question. It is very reassuring that the IR and Raman relative intensities calculated for these two bands are in good agreement with the observed intensity relations, too. The optimized values of the scaled force constants related to sulfur are: 3.50 N/m for the $C_{ar}-S$ bond stretch, 3.15 N/m for the $S-C_{methyl}$ bond stretch, and 1.68 N/m^2 for CSC bending. We believe that the final scale factors listed in Table 4 give better initial guesses for S-methyl compounds then the general 'heavy atom' factors given in Ref. [6].

Although the scale factors of the force field obtained with the large basis set are closer to unity than those obtained with the small basis, separate scale factors were needed for the sulfur vibrations at the B3LYP/6-311 + G** level as well to get a correct description of those modes. It is also interesting to note that, contrary to our expectations, the $S-C_{methyl}$ stretching mode does not give rise to a strong Raman band, at least not in this molecule; the strong Raman band found in the vicinity (at 673 cm^{-1}) is due to a ring deformation mode, with only 15% contribution from $C_{ar}-S$ stretching.

A common shortcoming of all calculations done with the small basis set is the significant difference between the observed and simulated IR and Raman intensity patterns in the 1500–1400 cm^{-1} region. It should be mentioned in this respect that the observed spectrum itself seems to be very sensitive in this region to changes in physical state of the sample as well, as one can see in Fig. 2(b) compared to Fig. 2(a). The large basis set performs much better in this sense in both IR and Raman spectra (compare Figs. 4(d) and 5(d) with 4(a) and 5(a), respectively).

5. Concluding remarks

Complete vibrational analysis of 2-(methylthio)benzonitrile was performed according to the SQM force field method based on DFT calculations at the B3LYP/6-31G* and B3LYP/6-311 + G** levels. Refinement of the scaling factors applied in this study achieved a weighted RMS deviation of 6.3 and 5.5 cm^{-1} for the small and large basis sets, respectively, between the experimental and SQM frequencies. The assignment of the fundamentals is confirmed by the qualitative agreement between the calculated and observed band intensities (especially with the large basis set) and polarization properties as well and is believed to be unambiguous.

Differences between uniform scaling and multiple scaling of the DFT force field and their influence on vibrational assignment were explored. The superiority of the SQM approach was confirmed by a better frequency fit

and a better agreement of the simulated and observed IR and Raman intensities as well, whereas introduction of independent scaling factors for sulfur-related force constants seems to be justified. The demonstrated corrections in assignment on selective scaling do not lead to spectacular changes in the simulated Raman spectrum, but in certain spectral regions the improvement is quite significant. The use of the larger basis set including more diffuse and polarization functions brings about further improvement in intensity calculations but we cannot speak of perfect spectrum simulations yet.

Acknowledgements

One of the authors (V.K.) is thankful to the Indian National Science Academy, New Delhi, for the award of a visiting fellowship to the Hungarian Academy of Sciences (HAS), Budapest, Hungary, under a bilateral exchange program. The computational facilities provided by the Chemical Research Center, HAS, and the instrumentation facilities provided by the RSIC, IIT Madras, Chennai are gratefully acknowledged. The authors are also thankful to Dr Sandor Holly for recording the vapor phase IR spectrum. This work has been supported in part by a research grant to G. K. (OTKA T-034776) from the Hungarian Scientific Research Fund.

References

[1] G. Socrates, Infrared and Raman Characteristic Group Frequencies—Tables and Charts, Third ed., Wiley, Chichester, 2001.
[2] E.B. Wilson Jr., J.C. Decius, P.C. Cross, Molecular Vibrations, McGraw Hill, 1955.
[3] P. Pulay, W. Meyer, J. Mol. Spectrosc. 40 (1971) 59.
[4] J.A. Pople, R. Krishnan, H.B. Schlegel, J.S. Binkley, Int. J. Quantum Chem. Symp. 13 (1979) 225.
[5] P. Pulay, G. Fogarasi, F. Pang, J.E. Boggs, J. Am. Chem. Soc. 105 (1983) 7037.
[6] G. Fogarasi, P. Pulay, in: J.R. Durig (Ed.), Vibrational Spectra and Structure, vol. 14, Elsevier, Amsterdam, 1985, pp. 125–219, Chapter 3.
[7] P. Pulay, G. Fogarasi, X. Zhou, P.W. Taylor, Vib. Spectrosc. 1 (1990) 159–165.
[8] G. Fogarasi, X. Zhou, P.W. Taylor, P. Pulay, J. Am. Chem. Soc. 114 (1992) 8191.
[9] P. Pulay, in: H.F. Schaefer III (Ed.), Application of Electronic Structure Theory, Modern Theoretical Chemistry, vol. 4, Plenum, New York, 1997, p. 153.
[10] A.P. Scott, L. Radom, J. Phys. Chem. 100 (1996) 16502.
[11] P. Pulay, J. Mol. Struct. 347 (1995) 293.
[12] A.D. Becke, J. Chem. Phys. 98 (1993) 5648.
[13] C. Lee, W. Yang, R.G. Parr, Phys. Rev. B. 37 (1998) 785.
[14] P. Pulay, G. Fogarasi, G. Pongor, J.E. Boggs, A. Vargha, J. Am. Chem. Soc. 105 (1983) 7037.
[15] G. Rauhut, P. Pulay, J. Phys. Chem. 99 (1995) 3093.
[16] J. Baker, A.A. Jarzecki, P. Pulay, J. Phys. Chem. A 102 (1998) 1412.
[17] Y.N. Panchenko, J. Mol. Struct. 567 (2001) 217.
[18] Y.N. Panchenko, G.R. De Maré, J. Mol. Struct. 611 (2002) 147.
[19] M. Belhakem, B. Jordanov, J. Mol. Struct. 218 (1990) 309.
[20] E.W. Thulstrup, J.H. Eggers, Chem. Phys. Lett. 85 (1968) 690.
[21] J. Michl, E.W. Thulstrup, Spectroscopy with Polarized Light. Solute Alignment by Photoselection, in Liquid Crystals, Polymers, and Membranes, VCH Publishers, New York, 1986, pp. 222–268, Chapter 5.
[22] M.J. Frisch, G.W. Trucks, H.B. Schlegel, P.M.W. Gill, B.G. Johnson, M.A. Robb, J.R. Cheeseman, T. Keith, G.A. Peterson, J.A. Montgomery, K. Raghavachari, M.A. Al-Laham, V.G. Zakrzewski, J.V. Ortiz, J.B. Foresman, J. Cioslowski, B.B. Stefanov, A. Nanayakkara, M. Challacombe, C.Y. Peng, P.Y. Ayala, W. Chen, M.W. Wong, J.L. Andres, E.S. Replogle, R. Gomperts, R.L. Martin, D.J. Fox, J.S. Binkley, D.J. Defrees, J. Baker, J.P. Stewart, M. Head-Gordon, C. Gonzalez, J.A. Pople, GAUSSIAN 94, Revision E.3, Gaussian Inc., Pittsburgh, PA, 1995.
[23] M.J. Frisch, G.W. Trucks, H.B. Schlegel, G.E. Scuseria, M.A. Robb, J.R. Cheeseman, V.G. Zakrzewski, J.A. Montgomery, Jr., R.E. Stratmann, J.C. Burant, S. Dapprich, J.M. Millam, A.D. Daniels, K.N. Kudin, M.C. Strain, O. Farkas, J. Tomasi, V. Barone, M. Cossi, R. Cammi, B. Mennucci, C. Pomelli, C. Adamo, S. Clifford, J. Ochterski, G.A. Petersson, P.Y. Ayala, Q. Cui, K. Morokuma, N. Rega, P. Salvador, J.J. Dannenberg, D.K. Malick, A.D. Rabuck, K. Raghavachari, J.B. Foresman, J. Cioslowski, J.V. Ortiz, A.G. Baboul, B.B. Stefanov, G. Liu, A. Liashenko, P. Piskorz, I. Komaromi, R. Gomperts, R.L. Martin, D.J. Fox, T. Keith, M.A. Al-Laham, C.Y. Peng, A. Nanayakkara, M. Challacombe, P.M.W. Gill, B. Johnson, W. Chen, M.W. Wong, J.L. Andres, C. Gonzalez, M. Head-Gordon, E.S. Replogle, J.A. Pople, GAUSSIAN 98, Revision A.11.4, Gaussian, Inc., Pittsburgh PA, 2002.
[24] T. Sundius, J. Mol. Struct. 218 (1990) 321.
[25] (a) T. Sundius, Vib. Spectrosc. 29 (2002) 89–95. (b) MOLVIB (v.7.0): Calculation of Harmonic Force Fields and Vibrational Modes of Molecules, QCPE program No. 807 (2002).
[26] P.L. Polavarapu, J. Phys. Chem. 94 (1990) 8106.
[27] G. Keresztury, S. Holly, J. Varga, G. Besenyei, A.Y. Wang, J.R. Durig, Spectrochim. Acta 49A (1993) 2007–2026.
[28] G. Keresztury, Raman spectroscopy: theory, in: J.M. Chalmers, P.R. Griffiths (Eds.), Handbook of Vibrational Spectroscopy, vol. 1, Wiley, 2002, pp. 71–87.
[29] G. Varsányi, Assignments for Vibrational Spectra of 700 Benzene Derivatives, vols. I–II, Akadémiai Kiadó, Budapest, 1973.
[30] F.R. Dollish, W.G. Fateley, F.F. Bentley, Characteristic Raman Frequencies of Organic Compounds, Wiley, New York, 1974, Chapter 5.